

This article was downloaded by:

On: 21 January 2011

Access details: *Access Details: Free Access*

Publisher *Taylor & Francis*

Informa Ltd Registered in England and Wales Registered Number: 1072954 Registered office: Mortimer House, 37-41 Mortimer Street, London W1T 3JH, UK



## The Journal of Adhesion

Publication details, including instructions for authors and subscription information:

<http://www.informaworld.com/smpp/title~content=t713453635>

### Predicted and Measured Bond-Line Read-Through Response in Composite Automotive Body Panels Subjected to Elevated Temperature Cure

H. Fuchs<sup>a</sup>; K. D. Fernholz<sup>b</sup>; P. Deslauriers<sup>c</sup>

<sup>a</sup> Multimatic Engineering, Livonia, Michigan, USA <sup>b</sup> Ford Motor Company, Dearborn, Michigan, USA <sup>c</sup> Multimatic Engineering, Markham, Ontario, Canada

Online publication date: 27 October 2010

**To cite this Article** Fuchs, H. , Fernholz, K. D. and Deslauriers, P.(2010) 'Predicted and Measured Bond-Line Read-Through Response in Composite Automotive Body Panels Subjected to Elevated Temperature Cure', *The Journal of Adhesion*, 86: 10, 982 – 1011

**To link to this Article:** DOI: 10.1080/00218464.2010.515471

**URL:** <http://dx.doi.org/10.1080/00218464.2010.515471>

PLEASE SCROLL DOWN FOR ARTICLE

Full terms and conditions of use: <http://www.informaworld.com/terms-and-conditions-of-access.pdf>

This article may be used for research, teaching and private study purposes. Any substantial or systematic reproduction, re-distribution, re-selling, loan or sub-licensing, systematic supply or distribution in any form to anyone is expressly forbidden.

The publisher does not give any warranty express or implied or make any representation that the contents will be complete or accurate or up to date. The accuracy of any instructions, formulae and drug doses should be independently verified with primary sources. The publisher shall not be liable for any loss, actions, claims, proceedings, demand or costs or damages whatsoever or howsoever caused arising directly or indirectly in connection with or arising out of the use of this material.

## Predicted and Measured Bond-Line Read-Through Response in Composite Automotive Body Panels Subjected to Elevated Temperature Cure

H. Fuchs<sup>1</sup>, K. D. Fernholz<sup>2</sup>, and P. Deslauriers<sup>3</sup>

<sup>1</sup>Multimatic Engineering, Livonia, Michigan, USA

<sup>2</sup>Ford Motor Company, Dearborn, Michigan, USA

<sup>3</sup>Multimatic Engineering, Markham, Ontario, Canada

*Visible distortions in automotive Class “A” surfaces, while being merely cosmetic defects, are unacceptable to customers. One type of surface distortion, referred to as bond-line read-through (BLRT), can occur due to the elevated temperature cure of an adhesive in bonded panel assemblies. The severity of these distortions can be measured by the local curvature of the surface. A finite element (FE) model capable of predicting the occurrence and severity of BLRT-induced surface distortions is being developed and validated. FE model predictions for the surface curvature of the outer panel in a bonded, laboratory scale assembly subjected to a simulated cool-down from the adhesive cure temperature to room temperature were compared with measured results. FE model predictions based on linear elastic material properties for the adhesive and substrate over-predicted the magnitude of the curvature in the outer panel as compared with the measured results. FE model predictions based on viscoelastic material properties for the adhesive and linear elastic material properties for the substrate resulted in substantially better correlation between predicted and measured distortions.*

**Keywords:** Bonded assemblies; Class “A” surface; Finite element modeling; Sheet molding compound; Surface distortion; Viscoelastic adhesive modeling

### INTRODUCTION

The aesthetic appearance of an automobile is one of the most important factors a customer considers when making a purchase decision. Consequently, automotive original equipment manufacturers

Received 13 November 2009; in final form 6 April 2010.

One of a Collection of papers honoring David A. Dillard, the recipient in February 2010 of the *Adhesion Society Award for Excellence in Adhesion Science, Sponsored by 3M*.

Address correspondence to K. D. Fernholz, Ford Motor Company, MD 3182/RIC, P.O. Box 2053, Dearborn, MI 48121. E-mail: kfernhol@ford.com

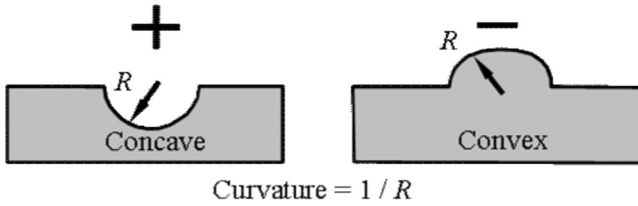


**FIGURE 1** Definition of positive and negative curvature.

(OEMs) work hard to ensure that all surfaces of an automobile are free of objectionable cosmetic defects and reflect the vehicle designer's intent. With the exception of some surface design features such as character lines, Class "A" exterior panels are designed to have smoothly varying surface curvatures. Any abrupt deviation from the design intent curvature can distort the appearance of the surface. These distortions can be perceived by customers as a cosmetic defect.

The severity of a surface distortion can be measured by the local curvature of the surface. Mathematically, the curvature is the second derivative of the displacement curve. In simple terms, the curvature of an arc is either concave or convex. A concave arc is defined to have positive curvature while a convex arc is defined to have negative curvature, as shown Fig. 1. If an arc is circular with a radius,  $R$ , the curvature of the feature is  $1/R$ .

Two types of deviations from the design intent surface curvature are illustrated in Fig. 2. The deviations shown in this figure are exaggerated for the purposes of this discussion. Distortions from

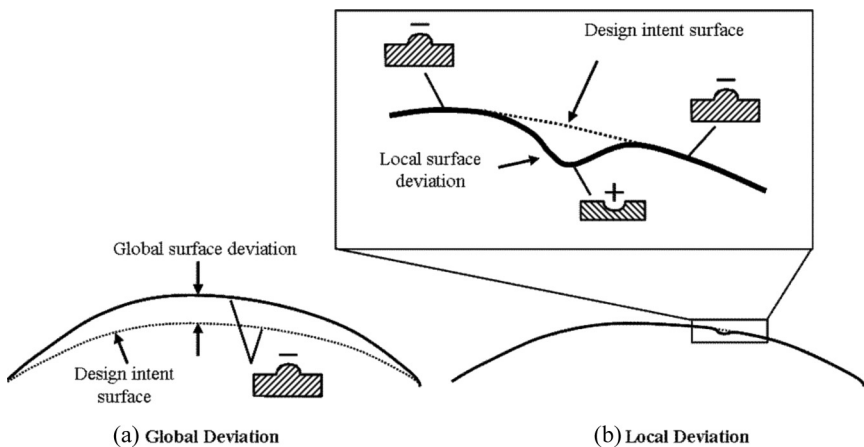


**FIGURE 2** Illustration of (a) global *versus* (b) local surface deviations.

design intent less than 10  $\mu\text{m}$  deep have been found to be visible in automotive exterior components [1].

The type of deviation illustrated in Fig. 2(a) is a “global deviation” while that illustrated in Fig. 2b a “local deviation.” A global surface deviation is a relatively subtle and uniform deviation from the general design intent of the surface and, therefore, is unlikely to be visible to a customer as long as the interface between adjoining panels is continuous and the gap between them is uniform. Conversely, a local surface deviation, as illustrated in Fig. 2b, is characterized by an abrupt change in curvature (from convex to concave to convex) over a short distance along the arc. This type of abrupt sign change in curvature has been found to be visible and objectionable to customers.

Visible surface distortions and the associated deviations in surface curvature can be caused by various manufacturing processes. In this work, only surface distortions due to elevated temperature cure of bonded Class “A” panel assemblies are considered. This particular type of distortion has been termed “bond-line read-through” (BLRT).

The typical solution to eliminating visible BLRT has been to increase the thickness of the assembly outer panel—essentially adding weight for appearance. Consequently, the Automotive Composites Consortium (ACC) has undertaken a multi-year project to develop a better understanding of the causes of this distortion. One objective of the project is to develop a validated finite element modeling methodology that can be used to predict the occurrence of BLRT before physical parts have been produced. This will allow designers and engineers to modify their designs to minimize BLRT-induced distortions before investing in prototype or production tooling. By ensuring that components have been designed to minimize these distortions, automotive OEMs will be able to minimize panel thickness, and the associated weight and cost, while meeting customer expectations for surface appearance quality.

Several factors are known to be the primary factors that determine the severity of BLRT-induced distortions. Reducing the temperature at which the adhesive is cured can eliminate the distortion [2]. The cross-sectional geometry of the adhesive bead has a significant effect on the severity of the distortions [3,4]. The relative stiffness and, coefficient of linear thermal expansion (CLTE) of with the adhesive compared with the substrate also play a significant role [4,5]. Finally, the bending stiffness and, therefore, thickness, of the outer panel and the local joint geometry can also influence the visibility of BLRT-induced distortions.

Varying degrees of BLRT-induced surface distortions can occur in assemblies built using any number of substrates and adhesives.

The primary objective of the ACC, however, is to increase the use of composites in automotive applications. Consequently, the majority of the assemblies built in this project have been built using panels molded from sheet molding compound (SMC). SMC is a class of composites consisting of polyester resin, glass fiber, calcium carbonate filler, and other additives. Some metal-metal and metal-SMC assemblies have also been produced to ensure that this phenomenon is fully understood and to understand potential limitations of the modeling strategy being developed.

The objective of the portion of the project discussed in this paper is to develop a finite element (FE) modeling strategy that can be used to predict the occurrence of BLRT-induced distortion and the magnitude of the resultant surface curvature. To determine whether the FE model correctly predicts the surface curvatures in an assembly, experimental data are compared with FE model predictions. The experimental data were collected *via* the ONDULO measurement system (Visuol Technologies, Metz, France) developed previously [6] and validated by the ACC over the course of several experiments to investigate the impact of various material and process factors on BLRT severity [2–5,7].

## BLRT MEASUREMENT

In the past, researchers have used altitude or slope to quantify the severity of BLRT-induced distortions [8–11]. Unfortunately, neither altitude nor slope are particularly good metrics for quantifying the visual severity of surface distortions. Altitude, in particular, does not necessarily correlate with one's visual assessment of the severity of a defect [12]. The contention of Hsakou [12] is that local surface curvature is the proper metric for measuring the visual severity of a defect. The authors have found that the magnitude of the curvature and the size of the defect correlate well with the perceived severity of BLRT-induced distortions. Thus, surface curvature is the primary component of the BLRT metric used in ACC work.

To illustrate the utility of using curvature data to identify and quantify the visual severity of surface distortions, ONDULO curvature data were acquired from a  $610 \times 610$  mm "free standing" Class "A" SMC panel with adhesive applied to the back (*i.e.*, non-Class "A") side. A photograph of the back side of that panel is shown in Fig. 3. Three epoxy adhesive patterns were hand-applied to the panel: 1) a continuous central bead, 2) five large drops, and 3) five small drops. The adhesive was cured by heating only the Class "A" side of the panel for 25 minutes at  $149^\circ\text{C}$ . The time required to cure the adhesive was

substantially longer than that required to cure this adhesive in an assembly since heat could only be applied from one side.

The primary output of the ONDULO technology [6] is a curvature map. A curvature map is a graphical representation of the curvature in the measured surface at each pixel in the image of the surface. An example of an unfiltered curvature map, obtained from the Class “A” surface of the freestanding outer panel shown in Fig. 3, is shown in Fig. 4.

In ONDULO curvature maps, curvature values close to zero are displayed as a medium gray color. As the curvature values increase in magnitude, the pixels become lighter (for large, positive curvature values) or darker (for large, negative curvature values). Because some surface characteristics do not affect one’s assessment of the visual severity of BLRT-induced distortions (*i.e.*, different defects have different “signatures” that can, in some cases, be decoupled), the data can be filtered to remove defects in the unrelated wavelengths. After filtering, the ACC has found that the mean curvature of a distortion must exceed  $\pm 0.3 \text{ m}^{-1}$  for that distortion to be visible on a black, high-gloss painted surface.

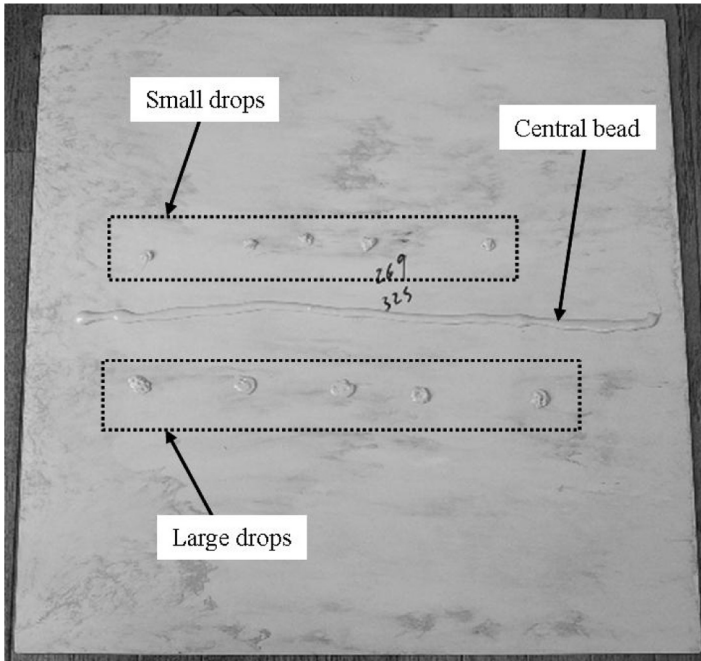


**FIGURE 3** Photograph of the back side of a freestanding SMC outer panel with epoxy adhesive applied.

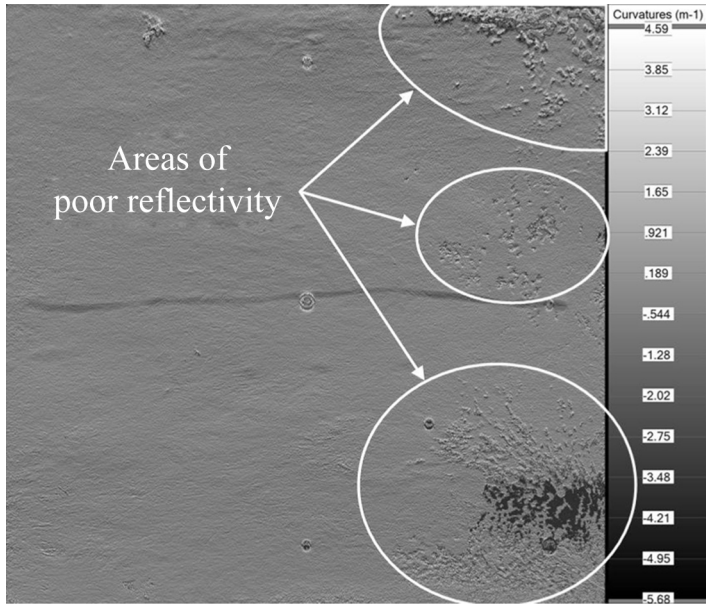


**FIGURE 4** Curvature map of the Class “A” surface of the panel in Figure 3 prior to filtering and masking.

The data in Fig. 4 are shown after having been filtered using the previously developed filtering process in Fig. 5. The reader should note that the scale used to display the curvature values in Fig. 5 ( $\pm 0.7 \text{ m}^{-1}$ ) is much smaller than the scale used in Fig. 4 ( $-5.68$  to  $+4.59 \text{ m}^{-1}$ ).

The ONDULO technology requires that a surface be reflective to obtain data. Typically, a clean, as-molded SMC surface is sufficiently reflective to provide high quality data. There can, however, be areas of low reflectivity on the SMC surface. If the reflectivity of the surface is poor there may be no data for that area or the data will be extremely noisy. Any area of the panel that has been sanded will not be reflective enough to provide good data. In addition, a residue from the molding process can be present on an SMC surface. That residue degrades the quality of the data wherever it is present. When measuring “raw” steel, highlighting oil must generally be applied to the surface to make the steel surface sufficiently reflective to obtain data. Unfortunately, great care must be taken to ensure that the oil is applied very thinly and evenly. Any streaks or bubbles in the oil will be detected as curvature variations and confound the data.

The Class “A” surface of the SMC panel shown in Fig. 3 had molding residue on portions of the surface; consequently, some areas were

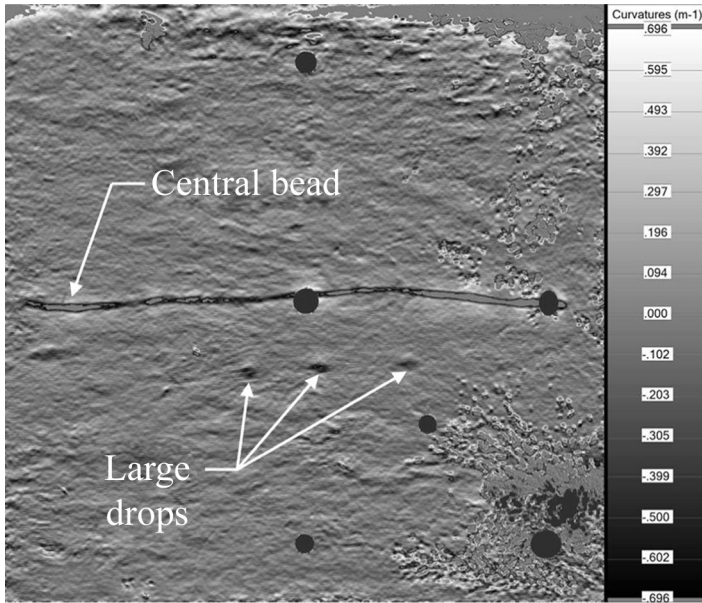


**FIGURE 5** Curvature map of the Class “A” surface of the panel in Figure 3 after filtering and masking.

unmeasured or exhibited excessive noise in the data. These areas are noted in Fig. 4 and can be seen in Fig. 5 as well. Fortunately, the regions of the panel that were not sufficiently reflective to acquire good quality data did not coincide with the locations to which adhesive was applied, so the curvature of the panel above the adhesive can still be measured.

The very dark circular or oval regions in Fig. 5 that are not present in Fig. 4 are areas where defects unrelated to BLRT (*e.g.*, molding defects, ejector pin mark-offs, etc.) were present. Because the curvature in those locations is not a result of BLRT-induced distortions, the data associated with those defects were removed from the data set by a masking operation. Masking of unrelated defects ensures that their presence does not confound the curvature variations due to BLRT-induced distortion.

A comparison of the areas of high curvature in the ONDULO curvature map in Fig. 5 with the adhesive locations shown in Fig. 3 shows that the light or dark areas in the curvature map correspond directly to the locations above the central bead and large drops of adhesive. Furthermore, comparison of ONDULO data with the physical panels



from which the data were captured has shown that locations of high positive and negative curvature correspond to the locations where distortion is visible on the Class "A" surface after painting<sup>1</sup>.

An analytical study [13] of the elevated temperature cure of a 9-mm wide  $\times$  4.5-mm high, centrally located epoxy adhesive bead on a 2.5-mm thick freestanding SMC panel, similar to the panel configuration shown in Fig. 3, provides additional insight into the utility of using curvature as a metric for quantifying the severity of distortions. The surface displacement, slope, and curvature in the surface of the panel after it has cooled to room temperature are shown in Fig. 6. The data in Fig. 6 correspond to a line transverse to the adhesive bead on the Class "A" surface above the epoxy adhesive bead in the center of the panel.

The displacements in Fig. 6 are plotted relative to a fixed reference point at the mid-span of the Class "A" surface of the freestanding panel. The displacement results indicate that a panel of this configuration will deform symmetrically downward about the centerline of the adhesive bead. The deformed shape of the panel is a result of the greater thermal shrinkage in the adhesive as compared with that in the SMC as the panel cools from cure temperature to room temperature. Note that the edges of the adhesive bead are not evident when looking at the displacements. The slope and the curvature results, however, do give an indication of the location of the edge of the adhesive bead. In addition, comparing the global curvature map shown in Fig. 5 with the calculated local curvature for the center of the bead cross section in Fig. 6, one can see that the measured curvature in the physical panel corresponds to a physical phenomenon that can be calculated based on material properties and specimen geometry, *i.e.*, the large negative curvature value at the center of the cross-section of the bead in Fig. 6 corresponds to the dark negative curvature line seen in the ONDULO curvature map in Fig. 5.

Both a) observational comparisons of the locations at which defects are visible on physical panels to the location and magnitude of regions of high curvature in a curvature map and b) the comparison of displacement (altitude), slope, and curvature profiles predicted by FE analysis support the authors' contention that curvature is the physical metric most well suited to quantifying the visual severity of distortions in Class "A" surfaces. Hence, curvature is used in this work to assess the severity of BLRT-induced surface distortions.

<sup>1</sup>Surface distortions are most visible on high gloss, black surfaces. As a result, distortions that will be visible after painting may be difficult to see visually prior to painting when the surface is a color other than black and has a lower gloss.

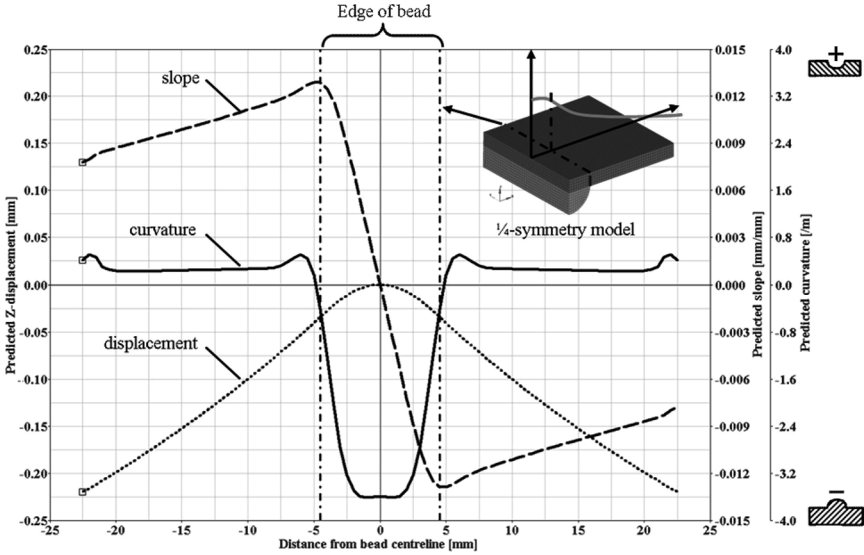


**FIGURE 6** Predicted displacement (altitude), slope, and curvature for an 2.5-mm thick SMC freestanding outer panel with an idealized 9-mm wide  $\times$  4.5-mm high epoxy adhesive bead (linear elastic analysis).

### Comparison of ONDULO and Profilometer Curvature Data

As noted previously, ONDULO data are necessarily filtered to remove unrelated data and to optimize the visualization of BLRT in the curvature maps. The ONDULO software provides a wide range of options for filtering the data. In the first phase of the ACC BLRT project, numerous filtering options were evaluated to determine which set of filters resulted in both the best visualization of the defects and the best correlation of BLRT “scores” with the subjective assessment of a jury of experts. To gain insight into how the selected filtering process might potentially affect the measured curvature magnitudes, very detailed altitude measurements were taken on a “lab-scale” assembly (discussed later in this paper) using an optical profilometer (UBM, Sunnyvale, CA, USA) with a resolution of  $0.05 \times 10^{-3}$  mm. Altitude data were acquired at a density of 500 points/mm across the nominally 15 mm width of the bead, and 4 points/mm along the length of the bead. To make the altitude data more tractable, it was re-sampled to a density of 50 points/mm and processed using a low pass filter to subjectively remove the high frequency noise content and to facilitate further post-processing. For comparison, the density of the ONDULO

data is significantly lower at a value of approximately 3 points/mm. The filtered profilometer altitude data were converted to slope and curvature data using the same finite difference scheme used with the FE displacement results shown in Fig. 6. Comparisons between profilometer- and ONDULO-based curvatures for representative SMC and steel samples are shown in Figs. 7 and 8, respectively, for a representative section transverse to the adhesive bead. For this analysis, an average of five adjacent line profiles on the separate bonded assemblies was calculated to provide additional assurance of the correlation between the two sets of measurements given the high level of noise in curvature data.

It is difficult to identify exactly the same location in both the profilometer data and in the ONDULO data to provide a definitive comparison of the data. Given that limitation, the results in both Figs. 7 and 8 indicate good agreement between the ONDULO and profilometer data in terms of the general shape of the feature and also the magnitude of the positive and negative peaks. The reader may note that the shape of the curvature profile for the steel assembly (Fig. 7) is different from that of the profile in the SMC assembly. The reason for this difference will be discussed later in the paper.

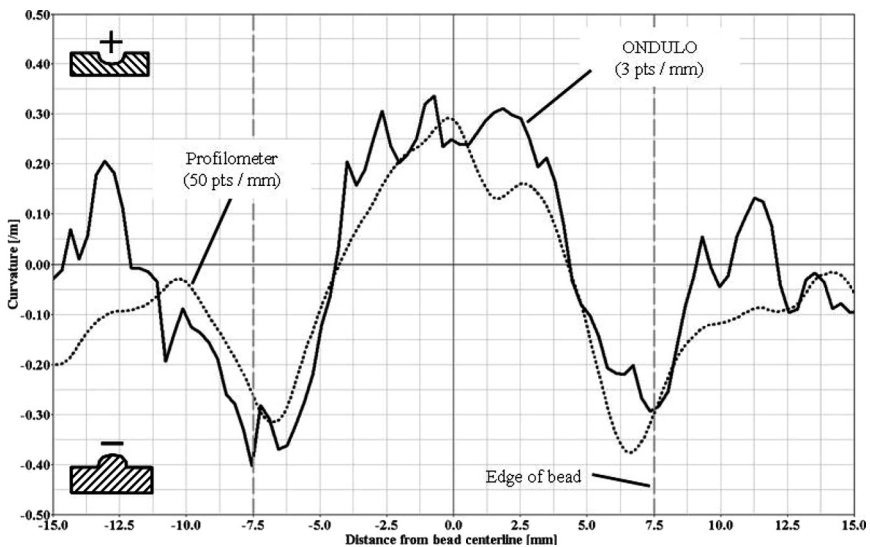


**FIGURE 7** Comparison of the curvature calculated from profilometer data with the ONDULO curvature values after filtering in an SMC lab-scale assembly.

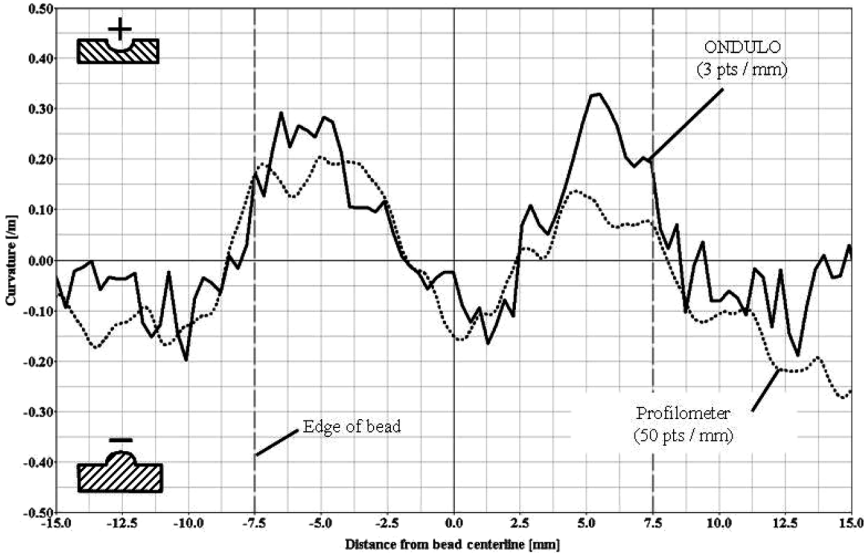


**FIGURE 8** Comparison of the curvature calculated from profilometer data with the ONDULO curvature values after filtering in a steel lab-scale assembly.

The reader may also note a significant amount of noise in the curvature data in Figs. 7 and 8. Curvature data are inherently noisy due to imperfections in the surface of the substrate. Any deviation from a perfectly flat surface will cause the local curvature to deviate from zero. SMC, even in formulations containing significant amounts of low profile additives, will never be perfectly flat due to differential shrinkage between the glass fibers, calcium carbonate, and polymer matrix. Similarly, the steel used in this project is coated to prevent corrosion and it is unreasonable to expect both that the steel itself was perfectly flat and that the coating was applied at a perfectly uniform thickness. Any of these variations will result in a non-zero “baseline” curvature in the surface. Furthermore, the application of oil to the steel surface to make it reflective enough to acquire data also contributes to the amount of noise in the data.

The fixturing used to position the samples to acquire ONDULO data can not position the panels precisely enough to allow assessment of the reproducibility of the curvature measurements on a pixel-by-pixel basis. In the case of the steel assemblies, any attempt to determine the reproducibility of the curvature measurement for an individual pixel would also be confounded by the application of oil

needed to make the measurement. If an assessment of repeatability and reproducibility of the ONDULO measurements is to be completed, it can only be completed using the “BLRT severity scores” discussed in [3]. That type of assessment has been completed; however, it is not reasonable to attempt to extrapolate the reproducibility of the pixel-by-pixel curvature measurements themselves from the reproducibility of this aggregate measurement.

When one takes into consideration the inherently high noise level in this type of data and the fact that the magnitude of the curvature induced by BLRT in Figs. 7 and 8 barely reaches the visible limit ( $0.3 \text{ m}^{-1}$ ), the comparison of the filtered ONDULO data with the data acquired by profilometer indicates that the filtering processes used to highlight the BLRT-induced curvature in the ONDULO data do not adversely affect the resulting magnitude of the data. The ONDULO data do tend to be noisier than the profilometer-based data in general, possibly as a result of the reduced data density or, in the case of the steel samples, as a result of the application of the highlighting oil. Nevertheless, these data indicate that the filtered ONDULO curvature measurements provide a dependable measure of the local curvature of the surface.

## EXPERIMENTAL PROCEDURE

Initial modeling demonstrated that BLRT is a highly localized phenomenon [13]. Consequently, a small lab-scale assembly was designed to allow the ACC to build assemblies from which ONDULO measurement data could be obtained to then compare with FE analysis predictions.

### Experimental Assembly Manufacture

Lab-scale assemblies consisted of a flat  $50 \times 197 \text{ mm}$  “inner panel” bonded to a  $133 \times 133 \text{ mm}$  “outer panel.” An image of a typical lab-scale assembly is provided in Fig. 9a. To obtain the SMC substrate for this experiment, nominally 2.5-mm thick plaques of standard density, Class “A” SMC (Magna Composites, Grabill, IN, USA) were molded using the ACC’s  $610 \times 610 \text{ mm}$  flat plaque compression mold (Service Mold, Windsor, Canada). Those plaques were then cut to the specified inner panel and outer panel dimensions. Similarly, steel substrate pieces of the specified size were cut from larger sheets of nominally 0.7-mm thick 210 bake-hardenable steel (AK Steel, West Chester, OH, USA). Three replicate assemblies were built with the SMC substrate and three were built with the steel substrate.

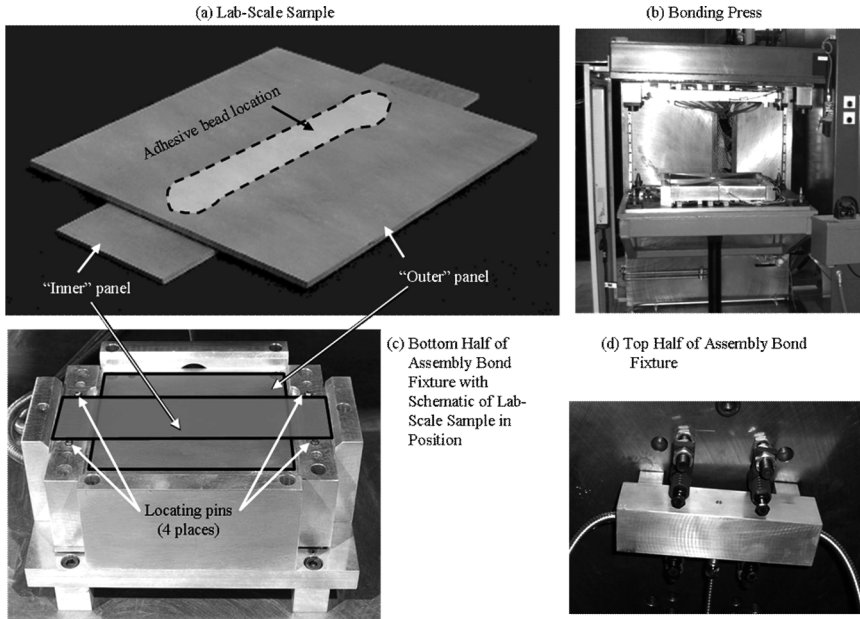


**FIGURE 9** (a) Lab-scale sample, (b) bonding press, (c) bottom half of assembly bonding fixture, and (d) top half of assembly bond fixture.

The two-part epoxy adhesive (Ashland Performance Materials, Dublin, OH, USA) used to bond these assemblies was robotically dispensed onto the outer panel. Prior to bonding the assemblies, the amount of adhesive required to produce a final bead with the target 15-mm width and 1-mm thickness was experimentally determined.

To simulate a typical automotive production manufacturing process, an electrically heated bonding fixture (EMC, Sterling Heights, MI, USA) was built to cure the assemblies. The fixture was actuated using a small bonding press (EMC). The fixture and press are shown in Figs. 9b–d. Shims were used in the bonding fixture and press to control the bond gap and to accommodate a range of panel thicknesses. The adhesive cure time was controlled by means of a timer on the bonding press.

The outer panel, with pre-applied adhesive, was placed in the bottom half of the bond fixture as shown in Fig. 9c. The inner panel was placed into the fixture on top of the adhesive bead between the locating pins. The assembly bond gap is controlled by the relative panel positions within the fixture. Once the assembly was in place, the bonding press was closed to initiate the curing cycle. Upon

reaching the prescribed cure time, the press automatically opened and the assembly was removed and allowed to cool at room temperature. All assemblies were cured in the bond press for 3 minutes at 149°C, per the adhesive manufacturer's recommendation.

## Data Acquisition

ONDULO curvature data were collected repeatedly on each sample to quantify the change in distortion on the panel over time. This was the first experiment in which data were collected on raw (*i.e.*, unpainted) steel assemblies. To obtain ONDULO data on raw steel, highlighting oil was applied to make the surface sufficiently reflective. Since the potential effects of applying highlighting oil to a hot steel assembly were unknown, data were not captured on these assemblies in the first 10 minutes after the assemblies were removed from the bond fixture to allow for sufficient cooling. The SMC assemblies, on the other hand, were sufficiently reflective as-molded, so data were captured on those assemblies immediately upon their removal from the fixture. Data were then collected according to the schedule given in Table 1. The total time required to acquire and process the measurement data for each sample was less than a minute.

It was observed that the highlighting process required to obtain data on raw steel assemblies could introduce extraneous features in the curvature measurements (Fig. 10a). Application of a minimal amount of oil free from drops or streaking minimized these extraneous features. In cases where the oil applied to the surface resulted in extraneous features in the data, the application process was repeated and the data were re-collected (Fig. 10b). Note also that the data in Fig. 10 show a) high levels of curvature at the edge of the panels and b) that the outer panel can be distorted by the spring-loaded pins used to hold it in place in the bond fixture. Those pins can be seen in Fig. 9d. To focus one's attention on the BLRT-related distortions, the data away from the bond-line will be cropped from the data sets in the following discussions.

**TABLE 1** Time After Bonding at Which Curvature Data was collected

Material	Immediately	5 min	10 min	15 min	30 min	1 hour	2 hours	4 hours	24 hours	2 wks*	3 wks	4 wks	6 wks
SMC	X	X	X	X	X	X	X	X	X	X	X	X	X
Steel	—	—	X	X	X	X	X	X	X	X	X	X	X

\*Samples were measured 5 days per week between 24 hours and 2 weeks.

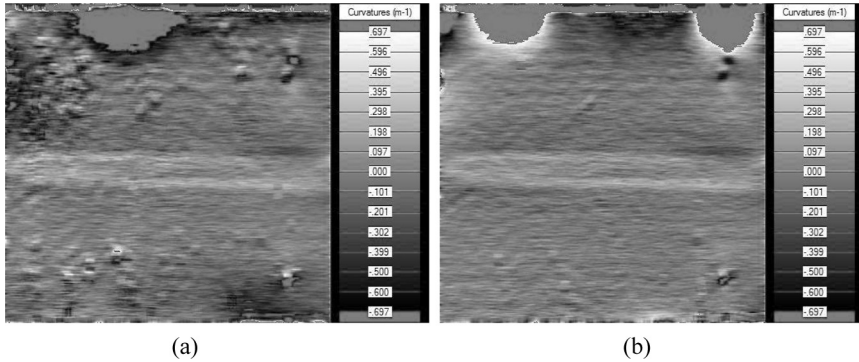


**FIGURE 10** Curvature maps for a raw steel assembly: (a) data obtained when highlighting oil is applied poorly, (b) data obtained when highlighting oil is applied well.

To obtain curvature data to compare with the FE predictions, the samples were aligned with the bond-lines parallel to one of the ONDULO scanning directions (*i.e.*, horizontal and vertical directions in Fig. 10). After collecting the measurements, curvature data were extracted from the appropriate ONDULO scan data along lines transverse to the bond-line near the central portion of the sample. An attempt was made to extract the curvature profile data from the same locations on each panel at each time interval. This was not always possible, however, since the position of the assembly shifted slightly from measurement to measurement. Consequently, the curvature profiles may be shifted slightly between measurements. To account for some of this potential variation, as well as the background noise level in the data, the average of five adjacent sections is compared with the FE predictions.

## MODELING APPROACH

The basic modeling approach was previously reported in [13]. A finite element model using solid elements was created for the lab-scale coupon geometry such that element edges were aligned parallel and perpendicular to the bond-line to facilitate a direct comparison of surface curvature results with the measured ONDULO and profilometer data. Surface curvatures were calculated from the predicted nodal displacements along a line transverse to the location of the adhesive bead using a simple finite difference scheme. Abaqus/Standard [14] was used as the finite element solver, and standard C3D8 fully integrated



linear brick elements were used to model the substrate and the adhesive. The nominal mesh size was  $0.5 \times 0.5 \times 0.5$  mm for the 2.5-mm thick SMC substrate,  $0.5 \times 0.5 \times 0.23$  mm for the 0.7-mm thick steel substrate, and  $0.5 \times 0.5 \times 0.33$  mm for the 1.0-mm thick adhesive bond-line. The nominal model thickness dimensions were adjusted slightly to represent more accurately the actual cross-section geometry of the specific coupons evaluated.

Thermo-mechanical analyses were conducted for the case of an idealized elevated-temperature adhesive cure with the nonlinear geometry option enabled. For this analysis, the panel was assumed to be stress-free at the elevated adhesive cure temperature, and the structural response was predicted for a specified temperature cool-down profile. The FE model setup and geometry details are shown in Figs. 11a–c, and the applied temperature profiles are shown in Fig. 11d. Note that the SMC temperature profile used during cool down was obtained by instrumenting an SMC lab-scale assembly with thermocouples located within the bond-line to acquire the *in-situ* temperature profile applied during the bonding cycle. A similar temperature profile was not available for the steel sample, so the temperature

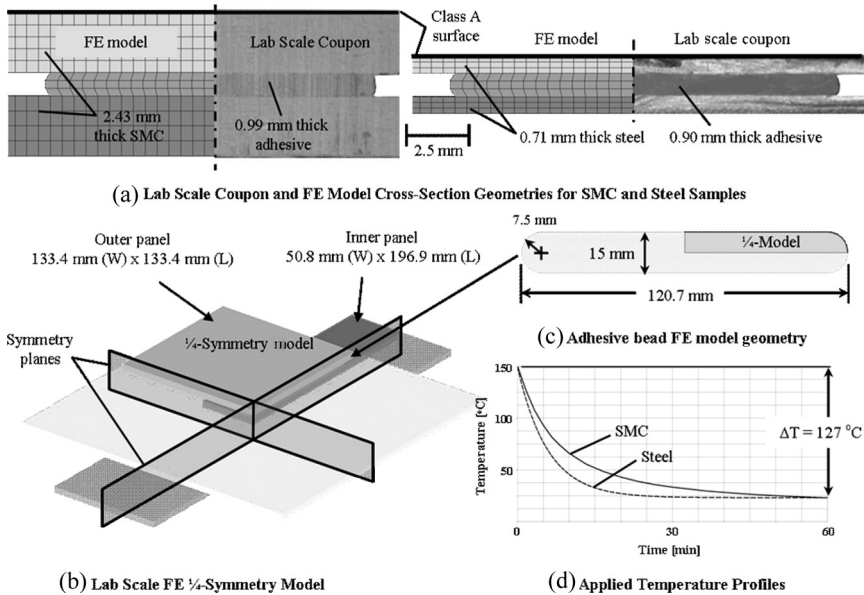


**FIGURE 11** (a) Lab-scale coupon and FE model cross-section geometries, (b) lab-scale FE  $\frac{1}{4}$ -symmetry model, (c) adhesive bead FE model geometry, and (d) applied temperature profiles.

**TABLE 2** Summary of Analysis Assumptions

Material	Analysis assumptions	
	Linear elastic	Viscoelastic
SMC	Elastic with temperature dependent properties	Elastic with temperature dependent properties
Steel	Elastic with constant properties	Elastic with constant properties
Epoxy adhesive	Elastic with temperature dependent properties	Viscoelastic with temperature dependent CLTE

profile was approximated by the application of Newton's law of cooling, assuming the same convective cooling rate for both SMC and steel. It was estimated from this calculation that the time for the steel sample to cool to room temperature was approximately one-half of the time required for the SMC sample. In the analyses, the applicable bond-line temperature profile was applied to all nodes in the model so that any local through-thickness or in-plane temperature gradients were ignored. A study of the transient thermal response for this coupon geometry showed this to be a reasonable assumption.

Both linear elastic and viscoelastic material property assumptions were evaluated for the adhesive. Those assumptions are summarized in Table 2. For the case of the analysis with viscoelastic adhesive material properties, an available linear isotropic viscoelastic material model was implemented using a Prony series representation and the Williams-Landel-Ferry equation for time-temperature superposition [14]. Viscoelastic effects for the SMC were not directly considered in the present paper due to the unavailability of a suitable orthotropic viscoelastic material model. Sensitivity studies were conducted to assess the potential effect of viscoelastic SMC behavior. It was assumed that the SMC through-thickness modulus,  $E_3$ , would be most affected by viscoelastic behavior and would diminish over time. The sensitivity studies found that directly reducing  $E_3$  resulted in reduced BLRT-induced curvature, while increasing  $E_3$  resulted in increased BLRT-induced curvature.

## Material Properties

The room temperature linear elastic properties used in the analysis are summarized in Table 3. The properties were synthesized from available test data and published values. Note that the SMC has orthotropic properties. The linear elastic temperature-dependent properties used in the FE analysis for the SMC and epoxy adhesive

**TABLE 3** Room Temperature Linear Elastic Material Properties used for FEA

Property	Units	SMC	Steel	Epoxy
<b>Modulus</b>				
$E_1$	Gpa	10.6		
$E_2$	Gpa	13.7	207	3.30
$E_3$	Gpa	6.0		
<b>Poisson's Ratio</b>				
$\nu$	--	0.25	0.29	0.49
<b>Density</b>				
$\rho$	g/cc	1.9	7.8	1.32
<b>Coefficient of Linear Thermal Expansion (CLTE)</b>				
$\alpha_1, \alpha_2$	$10^{-6}/^\circ\text{C}$	11.0	14.0	94.8
$\alpha_3$	$10^{-6}/^\circ\text{C}$	40.0		

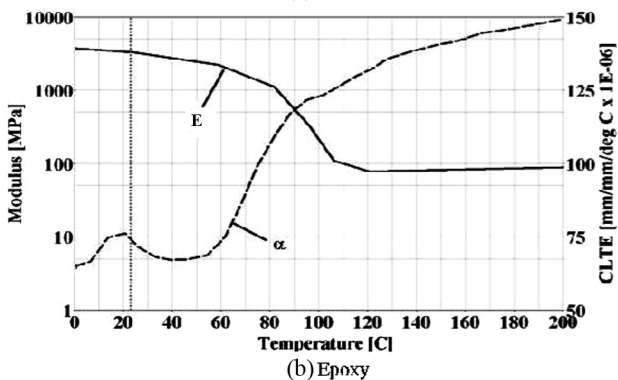
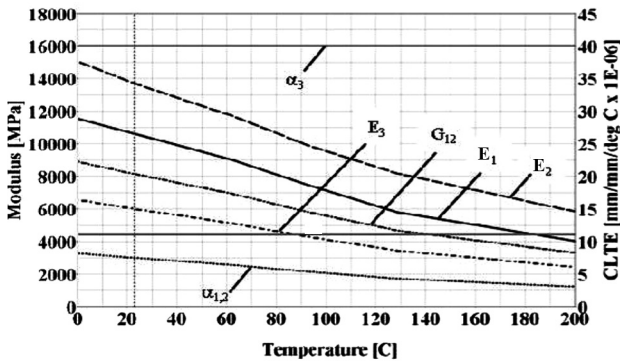
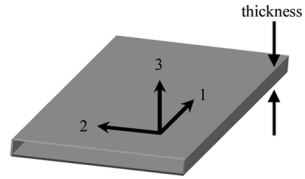


**FIGURE 12** Temperature-dependent linear elastic moduli and CLTE assumptions for (a) SMC and (b) epoxy adhesive.

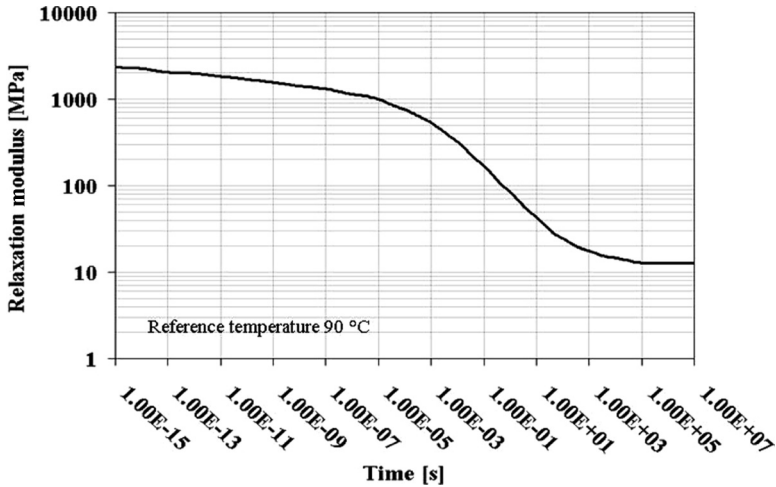


**FIGURE 13** Prony series stress relaxation master curve representation for viscoelastic epoxy adhesive.

are shown in Fig. 12. The adhesive CLTE data in Fig. 12 were based on test data [15]. The properties for steel were assumed to be linear elastic and constant over the temperature range of interest. In the case of viscoelastic analyses, the relaxation modulus of the epoxy adhesive was represented by a 20-term Prony series shown in Fig. 13, while the CLTE was represented by the temperature dependent response shown in Fig. 12. The Prony series viscoelastic adhesive characterization was based on stress relaxation test data [15].

## RESULTS

### Experimental Results

Figure 14 shows selected curvature maps for an SMC assembly and a steel assembly over a period of time from immediately after removal from the bond fixture up to 6 weeks later. The data away from the bond-line have been cropped to highlight the area of interest around the bond-line.

The first thing to note in Fig. 14 is that there was no BLRT-induced distortion present in the SMC assembly immediately after that assembly was removed from the bond fixture. The distortion was then essentially fully formed for both assemblies within 15 minutes of being removed from the bond fixture. The distortion did continue to increase slightly in magnitude after 15 minutes as the assembly continued to cool to room temperature. Careful study and comparison of the

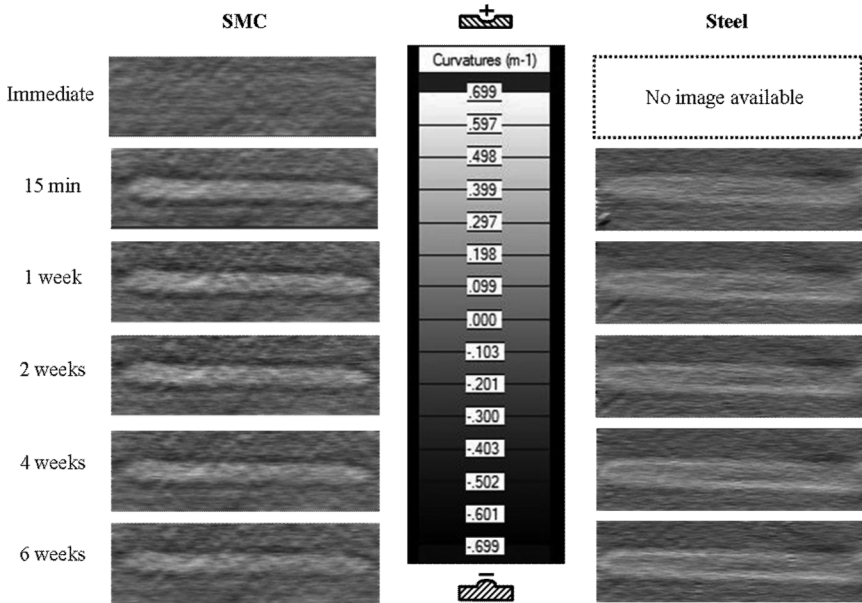


**FIGURE 14** Curvature maps for SMC and steel assemblies bonded with epoxy at varying times after bonding (immediate to 6 wks).

curvature maps provided in Fig. 14 shows a subtle reduction in the peak negative curvature over time in both the SMC and steel assemblies. This reduction in peak negative curvature is visible as a change in the gray level of the pixels around the edge of the bead from dark gray to lighter gray. Unfortunately, changes that can be perceived when one compares the data in curvature map form (*i.e.*, a global change) become much more difficult to discern when comparing curvature values extracted along a line through the data (*i.e.*, a local change).

Figure 15 shows a comparison of the measured curvature along a transverse section across the bond-line in an SMC assembly at 15 minutes after bonding and 6 weeks after bonding. The data in Fig. 15 appear to indicate there was no change in BLRT-severity over time. This seems to contradict the observed reduction in severity in the global data shown in Fig. 14. This difference between the apparent stability of BLRT over time in the local data as compared with the global data is likely due to a) the amount of noise inherent in curvature data and b) the difficulty in identifying the exact same location in the curvature map for each subsequent measurement. In addition, the BLRT-induced curvature in these particular specimens was very small. All of these facts make correlation between the experimental

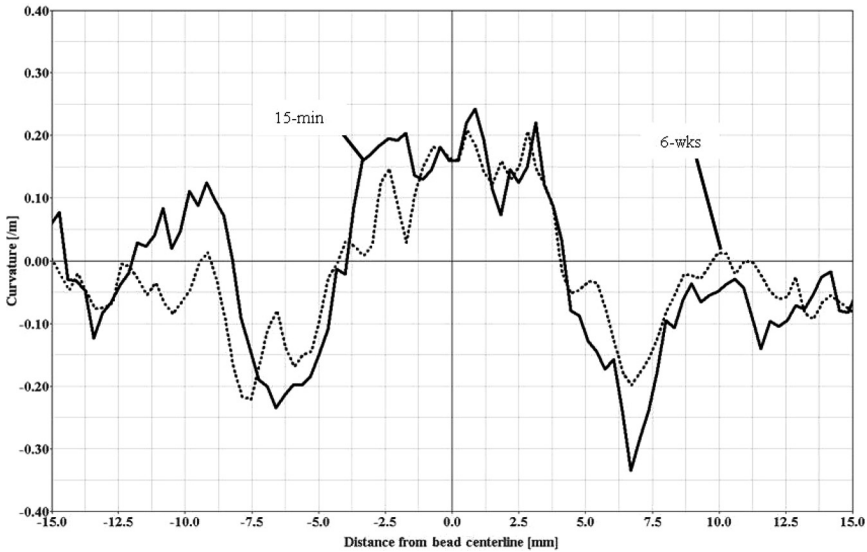


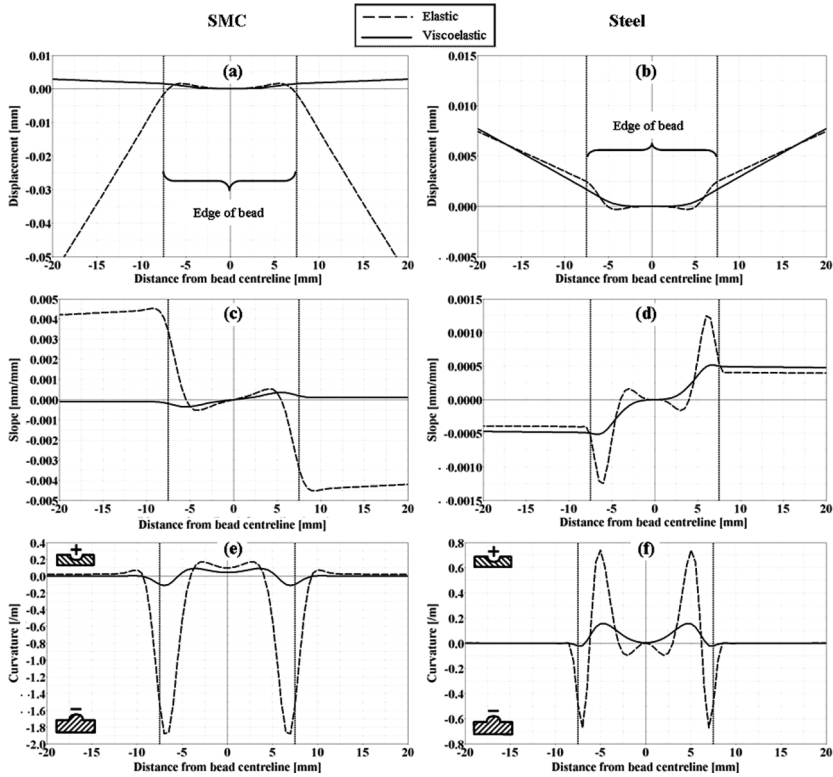
**FIGURE 15** Comparison of measured curvature over 6 weeks in the region of the bond-line for an SMC assembly bonded with epoxy.

data and modeling predictions more difficult. The authors contend that trends predicted by the model can be compared with the trends evident in the global curvature maps while the local line profile data can be used to validate the predicted curvature magnitudes.

Figure 15 shows that the peak curvature values in these assemblies reached  $\pm 0.3 \text{ m}^{-1}$  in very limited areas. This indicates that these distortions would, at most, be barely visible on a highly reflective, black surface. Given that the SMC and steel surfaces were gray and not particularly high gloss, the BLRT on these assemblies was not visible to the unaided eye.

### Model Response Predictions

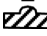
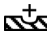
FE analyses were performed for both the SMC and steel assemblies described in Fig. 11 using the linear elastic and viscoelastic analysis assumptions outlined in Table 2. The linear elastic and viscoelastic displacement, slope, and curvature responses for these cases are compared in Fig. 16 for the SMC and the steel assemblies after a 1 hour,  $127^\circ\text{C}$  cool-down to room temperature. Note that different scales are used to plot the results for the SMC and steel assemblies to highlight the individual responses.



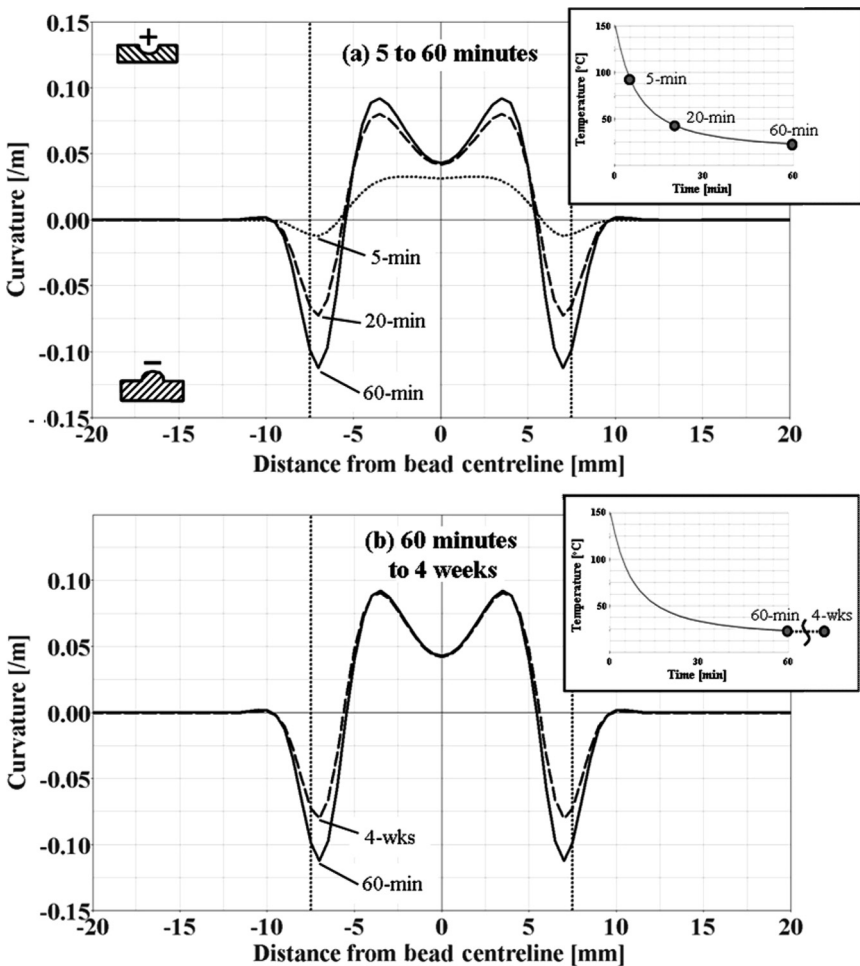
**FIGURE 16** (a, b) Comparison of predicted elastic and viscoelastic surface displacement, (c, d), slope and (e, f) curvature responses for SMC and steel assemblies 1 hour after cure.

The responses observed for the bonded SMC assemblies in Fig. 16 are different from those observed for the steel assemblies. The displacement results indicate that the SMC outer panel is predicted to

**TABLE 4** Peak Curvature Comparison at 1 Hour for Linear and Viscoelastic Adhesive

	SMC			Steel		
	Elastic	Viscoelastic	% Reduction	Elastic	Viscoelastic	% Reduction
Peak	curvature [1/m]		%	curvature [1/m]		%
Negative 	-1.878	-0.112	94	-0.672	-0.022	97
Positive 	0.169	0.092	46	0.739	0.156	79

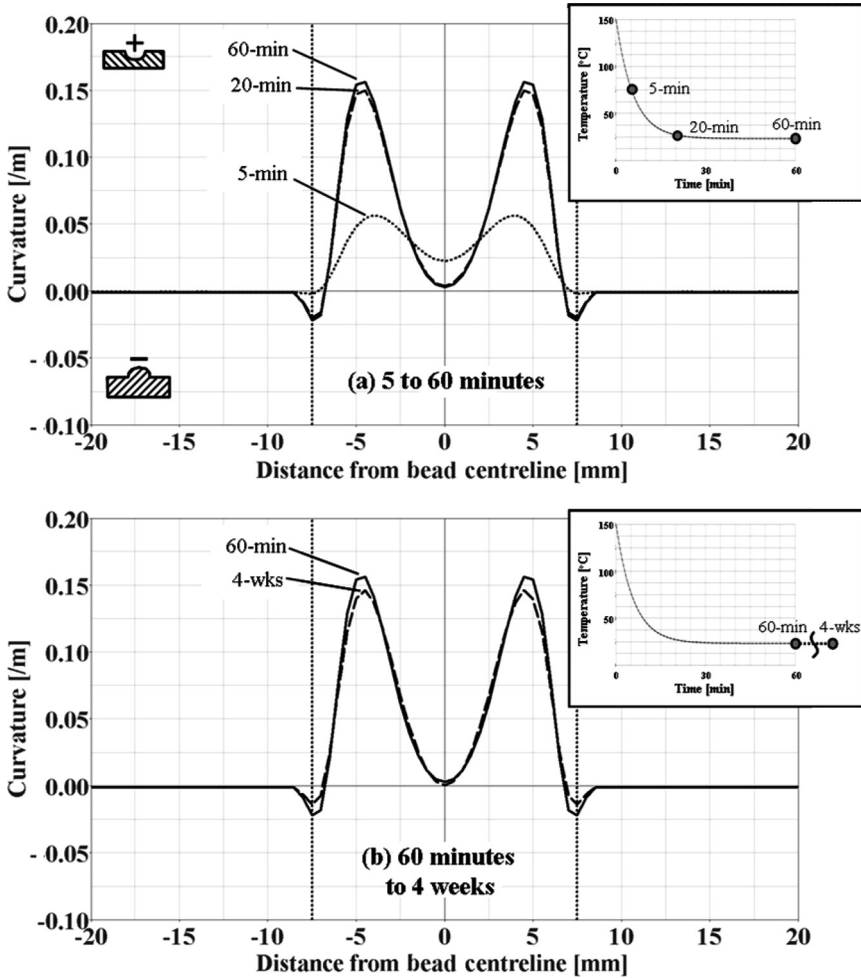
bend downward locally just inside the edge of the adhesive bead (Fig. 16a), while the steel panel is predicted to bend upward (Fig. 16b). The maximum slope occurs outside the edge of bead for the SMC panel (Fig. 16c), while it occurs inside the edge of bead for the steel panel (Fig. 16d). The peak curvature for both assemblies occurs just inside the edge of bead; however, the peak curvature for the SMC panel is negative (Fig. 16e), while the peak curvature for the steel panel is positive (Fig. 16f). Viscoelastic



**FIGURE 17** SMC – predicted progression of (a) curvature build-up during cool-down (5–60 min) and (b) curvature relaxation after cool-down to room temperature (60–4 wks).

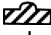



adhesive properties result in a significant reduction in the localized bending near the edge of the bead. This greatly diminishes the peak slope and curvature values predicted as compared with that predicted using linear elastic assumptions. The predicted peak linear elastic and viscoelastic curvatures values are compared in Table 4. The peak curvature results show that the SMC assembly is predicted to have larger negative peak curvature values than



**FIGURE 18** Steel – predicted progression of (a) curvature build-up during cool-down (5–60 min) and (b) curvature relaxation after cool-down to room temperature (60–4 wks).

**TABLE 5** Viscoelastic Adhesive Peak Curvature Comparison for 1 Hour and 4 Weeks

	SMC			Steel		
	Viscoelastic, 1 hr	Viscoelastic, 4 wks	% Reduction	Viscoelastic, 1 hr	Viscoelastic, 4 wks	% Reduction
Peak	curvature [1/m]		%	curvature [1/m]		%
Negative 	-0.112	-0.080	29	-0.022	-0.014	37
Positive 	0.092	0.091	2	0.156	0.146	7

the steel assembly, but smaller positive peak values. Significant reductions in the peak curvatures are predicted for the case of a viscoelastic adhesive, with an approximately 95% reduction in negative curvature for both assemblies, and 46 and a 79% positive peak reduction for SMC and steel, respectively.

The predicted progression of curvature build-up during cool-down to room temperature and subsequent relaxation due to the viscoelasticity of the adhesive are shown in Fig. 17 for the SMC assembly, and in Fig. 18 for the steel assembly. The figures show how the peak curvatures build to their maximum value during the 1 hour cool-down, and subsequently relax over a period of 4 weeks. The relaxation in peak curvature that is predicted to occur from a time period of 1 hour to 4 weeks after bonding is summarized in Table 5. The results indicate a 29 and 37% reduction in the negative peak curvature for SMC and steel, respectively. In comparison, only a 2 and 7% reduction in the positive peak curvature is predicted for SMC and steel, respectively. In comparing peak curvature values for both panels, the SMC assembly is predicted to have a larger negative peak and a smaller positive peak than the steel assembly. Experience has shown that additional BLRT peak curvature reduction can occur as a result of subsequent paint bake cycles. This change in BLRT severity as a result of typical subsequent processing is not considered in the present paper.

## DISCUSSION

### Comparison of the Modeling and Experimental Results

The predicted curvature responses are compared with ONDULO curvature data for an SMC assembly in Fig. 19 and for a steel assembly in Fig. 20. The FE analysis predictions are shown based on viscoelastic material properties at a time of 60 minutes and 4 weeks.

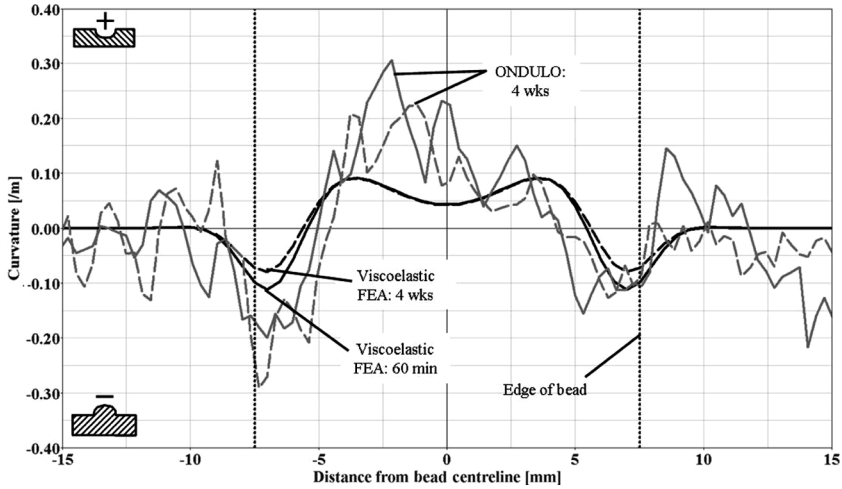


**FIGURE 19** Comparison of measured and predicted BLRT curvatures at a typical bond-line section for an SMC assembly.

The ONDULO curvature data are shown for two representative adhesive cross-sections at 4 weeks after bonding. The reader should reference Fig. 16 to compare these FE analysis predictions with the predicted curvature responses based on linear elastic material property assumptions.

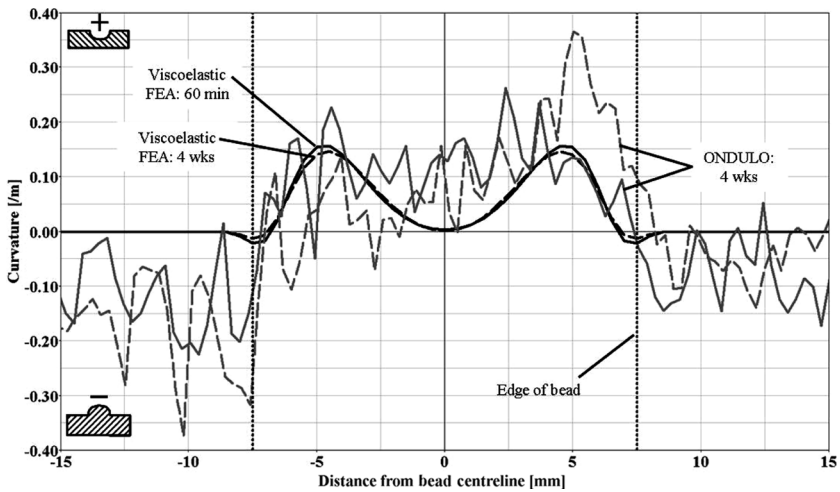


**FIGURE 20** Comparison of measured and predicted BLRT curvatures at a typical bond-line section for a steel assembly.

The SMC assembly results shown in Fig. 19 demonstrate that the implementation of viscoelastic adhesive properties results in good agreement with the measured data in terms of the curvature amplitude and overall shape of the response. This agreement is considerably improved relative to the linear elastic responses shown in Fig. 16, which significantly over-predict the severity of the negative peak BLRT curvature. Although there is a 29% reduction in the predicted negative peak between the 1 hour and 4 week viscoelastic response, this difference is small relative to the noise in the experimental data.

Similar to the SMC assembly results, the steel assembly results shown in Fig. 20 again demonstrate that the implementation of viscoelastic adhesive properties results in good agreement with the measured data in terms of the curvature amplitude and general shape of the response. This agreement is also considerably improved relative to the linear elastic responses shown in Fig. 16, which significantly over-predict the severity of the positive and negative peak BLRT curvatures.

The curvature magnitude caused by the BLRT-induced distortions in these particular assemblies was relatively small. As such a) the distortions were unlikely to be visible even if the assemblies had been painted and b) the magnitude of the resultant surface curvature was not much larger than the magnitude of the noise in the data. Additional experiments using modified lab scale coupons are planned to generate higher levels of BLRT to better distinguish the BLRT curvature data from the ambient noise levels and further validate the current modeling approach.

## **SUMMARY**

A study was conducted to evaluate the ability of a FE model to predict the BLRT response of bonded automotive body panels subjected to elevated temperature cure. For the experimental part of the study, SMC and steel lab-scale assemblies were bonded and cured at an elevated temperature using an electrically heated bonding fixture. The ONDULO technology was used to characterize the surface curvature of the samples over a period of time spanning from immediately after bonding to 6 weeks after bonding. The ONDULO curvature data were also compared with curvature data derived from detailed optical profilometer measurements to evaluate the effect of the filtering methodology used to make the BLRT response in the ONDULO data more clearly visible and to make the numerical BLRT severity scores better correlated with visual assessments. Curvature data were extracted from the ONDULO data transverse to the adhesive bead for the

purpose of comparing the measured response with the analysis predictions. The curvature maps for the SMC assemblies show a pronounced line of negative curvature around the perimeter of the bond-line. This negative curvature was not present immediately after the assembly was removed from the bond fixture, but had appeared within 15 minutes after the assemblies had been removed. The magnitude of the negative peak appeared to relax slightly over a period of 6 weeks. The measured curvature maps for the steel samples showed a less pronounced negative curvature peak around the outside of the adhesive bead as compared with that seen in the SMC samples as well as a more pronounced region of positive curvature within the perimeter of the bond-line.

For the analytical part of the study, a detailed FE model was created to simulate the geometry and the materials used to build the bonded assemblies. An applied temperature profile derived from measured data was used to drive the thermo-mechanical analyses. Results were provided for two material property scenarios: a) temperature-dependent linear elastic adhesive and substrate material properties, and b) temperature-dependent linear elastic substrate and viscoelastic adhesive material properties. Linear elastic properties were synthesized based on available test data and published data. Viscoelastic adhesive properties were based on a stress relaxation characterization and a Prony series representation which was implemented in a commercially available FE solver. Analysis predictions were compared for both sample constructions to understand the differences in displacement, slope, and curvature responses. Both samples were predicted to exhibit thermally induced local bending just inside of the edge of the bead, with the SMC panel bending in a direction opposite to that of the steel panel. The consideration of a viscoelastic adhesive considerably reduced the predicted localized bending of the outer panel, and the corresponding peak surface curvatures were reduced by up to 97% relative to the linear elastic value.

Curvature results from the analysis were directly compared with data extracted from ONDULO measurements of the experimental assemblies. The overall shape of the predicted curvature response agreed well with the measured results for both SMC and steel assemblies. The results predicted for the case of linear elastic material property assumptions significantly over-predicted the magnitude of the ONDULO curvatures. By comparison, the results predicted for the case of the viscoelastic adhesive material property assumptions was found to agree well with the ONDULO curvatures, given the level of noise observed in the data.

## CONCLUSIONS

A comparison between curvature derived from a detailed profilometer scan and data extracted from ONDULO measurements after application of the filtering processes developed as part of this project indicated good agreement between both the nature of the curvature response and the peak curvature values, thus validating the ONDULO methodology used.

The experiments showed a build-up of BLRT-induced distortion in the surface of an assembly as it cooled after being removed from the bond fixture. The distortion induced in these particular assemblies was relatively small with peak curvature values at, or below, the established visible threshold. The BLRT was not visible to the unaided eye on the assemblies as bonded and would have been only minimally visible had the assemblies been painted. Fortunately, the ONDULO measurements are more sensitive than the human eye and BLRT was clearly evident in the ONDULO data for both the SMC and steel assemblies. The BLRT appeared to fade slightly over a period of 6 weeks.

The analysis model correctly captured the character of the measured curvature response for two different substrates, even though the response was different for the two different substrates. The effect of the viscoelastic nature of the adhesive was significant and must be accounted for in the analysis to predict the response accurately. Further, the model captured the initial build-up of curvature that occurred during cool-down after bonding and the subsequent relaxation over time. However, a detailed quantitative comparison is difficult due to the noise level of the measured data. Further work is underway to generate higher levels of BLRT in laboratory coupons to further validate the modeling approach and material properties; however, the present results and level of correlation are very encouraging.

Because the painting process affects both the severity of BLRT-induced distortions and the visibility of these distortions, the effect of painting processes will need to be considered in the future so that manufacturers do not devote their valuable resources trying to reduce distortions that a customer will never see. Whether the model is capable of accounting for the effect of painting processes is yet to be evaluated.

## ACKNOWLEDGMENTS

This material is based upon work supported by the Department of Energy National Energy Technology Laboratory under Award Number DE-FC26-02OR22910.

This report was prepared as an account of work sponsored by an agency of the United States Government. Neither the United States Government nor any agency thereof, nor any of their employees, makes any warranty, express or implied, or assumes any legal liability or responsibility for the accuracy, completeness, or usefulness of any information, apparatus, product, or process disclosed, or represents that its use would not infringe privately owned rights. Reference herein to any specific commercial product, process, or service by trade name, trademark, manufacturer, or otherwise does not necessarily constitute or imply its endorsement, recommendation, or favoring by the United States Government or any agency thereof. The views and opinions of authors expressed herein do not necessarily state or reflect those of the United States Government or any agency thereof.

## REFERENCES

- [1] Andersson, A., *J. Materials Processing Technology* **209**, 821–837 (2009). doi:10.1016/j.jmatprotec.2008.02.078
- [2] Fernholz, K. D. and Lazarz, K., *The 33rd Annual Meeting of the Adhesion Society*, Daytona Beach, FL, 21–24 Feb. (2010), pp. 211–213.
- [3] Fernholz, K. D., Lazarz, K., and Wang, C. S., *The 32nd Annual Meeting of the Adhesion Society*, Savannah, GA, 15–18 Feb. (2009), pp. 285–287.
- [4] Fernholz, K. D., Fuchs, H., Deslauriers, P., Lazarz, K., and Wang, C. S., *COMPOSITES 2010*, Las Vegas, NV, 9–11 Feb. (2010).
- [5] Fernholz, K. D., Lazarz, K., and Wang, C. S., *SPE Automotive Composites Conference*, Troy, MI, 15–16 Sept. (2009).
- [6] Fernholz, K. D., Hsakou, R., Lazarz, K., Wang, C. S., Emerson, B., Biernat, D., and Case, D., *SPE Automotive Composites Conference*, Troy, MI, 11–13 Sept. (2007).
- [7] Fernholz, K. D., Blair, B., Wang, C. S., and Lazarz, K., *SPE Automotive Composites Conference*, Troy, MI, 16–18 Sept. (2008).
- [8] Durso, S. R., Howe, S. E., and Pressley, M. W., Adhesive Bond-line Read-through: Theoretical and Experimental Investigation, *SAE Technical Paper Series*, SAE-1999-01-0984, (1999).
- [9] Lee, C. C., *J. Reinforced Plastics & Composites* **14** (11), 1226–1249 (1995).
- [10] Hahn, O. and Jendry, J., *Welding In The World* **47** (7–8), 31–38 (2003).
- [11] Basu, S. K. and Kia, H. G., *J. Composite Materials* **42** (6), 539–552 (2008).
- [12] Hsakou, R., *JEC Composites Magazine*, No. 23, 105–108 (2006).
- [13] Fuchs, H. and Deslauriers, P., *SPE Automotive Composites Conference*, Troy, MI, 15–16 Sept. (2009).
- [14] Anonymous, Abaqus Version 6.8EF User's Manual, Dassault Systèmes, 2008.
- [15] Dillard, D., ACC Testing Contract, "Characterizing the Viscoelastic and Thermal Properties of Adhesives for Modeling Bondline Readout," Virginia Tech, Blacksburg, VA, June 2009.